

## Dissociation of Energy-selected $c\text{-C}_2\text{H}_4\text{S}^+$ to Form $\text{CH}_3\text{CS}^+ + \text{H}$ and $\text{HCS}^+ + \text{CH}_3$ : TPEPICO Experiments and G3 Calculations

### Beamline

04B1 Seya/Gas Phase beamline

### Authors

S.-Y. Chiang and I-Feng Lin  
National Synchrotron Radiation  
Research Center, Hsinchu, Taiwan

*Dissociation of energy-selected  $c\text{-C}_2\text{H}_4\text{S}^+$  to form  $\text{CH}_3\text{CS}^+ + \text{H}$  and  $\text{HCS}^+ + \text{CH}_3$  was investigated with threshold photoelectron-photoion coincidence experiments and Gaussian-3 calculations. The measured average releases of kinetic energy for channel  $\text{CH}_3\text{CS}^+ + \text{H}$  of least energy are substantial and much greater than those calculated with quasi-equilibrium theory; in contrast, small releases of kinetic energy near the appearance onset for channel  $\text{HCS}^+ + \text{CH}_3$  agree satisfactorily with statistical calculations. The large releases of kinetic energy might result from a dissociation mechanism according to which  $c\text{-C}_2\text{H}_4\text{S}^+$  isomerizes to a local minimum  $\text{CH}_3\text{CSH}^+$  and then dissociates through a transition state to form  $\text{CH}_3\text{CS}^+ + \text{H}$ . A predicted dissociation mechanism that  $c\text{-C}_2\text{H}_4\text{S}^+$  isomerizes to  $\text{CH}_3\text{CHS}^+$  before dissociating to linear  $\text{HCS}^+ + \text{CH}_3$  supports the experimental results.*

State-selected chemistry has gained great interests in the investigation of dynamics of ion dissociation and of ion-molecular reactions in the past decades because of valuable information on branching ratios, partitions of kinetic energy released and internal energies, dissociation and reaction rates at a specific energy level. Various techniques with a laser, discharge lamp or synchrotron radiation as light source, such as multiphoton ionization (MPI) and coincidence methods, have been developed for state-selected studies. Threshold photoelectron photoion coincidence (TPEPICO) that allows one to study dissociation mechanisms of a molecular ion prepared in a well-defined energy state has been proved to be one of the powerful tools. In this highlight, we report the dissociation of energy-selected  $c\text{-C}_2\text{H}_4\text{S}^+$  into channels  $\text{CH}_3\text{CS}^+ + \text{H}$  and  $\text{HCS}^+ + \text{CH}_3$  studied with a molecular beam/threshold photoelectron-photoion coincidence system and with Gaussian-3 (G3) calculations.

Thiirane ( $c\text{-C}_2\text{H}_4\text{S}$ ) attracts fundamental interest as its large ring strain facilitates ring-opening processes and isomerization upon photoexcitation. The photochemistry of  $c\text{-C}_2\text{H}_4\text{S}$  is also of fundamental importance as photodissociation or photoionization of  $c\text{-C}_2\text{H}_4\text{S}$  offer a powerful means to produce reactive HCS or  $\text{HCS}^+$  that plays an important role in atmospheric chemistry and serves as a prototypical system in the chemistry of sulfur-containing organic compounds. We have investigated the dissociative photoionization of molecular-beam-cooled  $c\text{-C}_2\text{H}_4\text{S}$  in a region  $\sim 9 - 20$  eV with a photoionization mass spectrometer coupled to a synchrotron radiation as an ionization source. Five major fragment ions –  $\text{C}_2\text{H}_3\text{S}^+$ ,  $\text{C}_2\text{H}_2\text{S}^+$ ,  $\text{HCS}^+$ ,  $\text{H}_2\text{S}^+$  and  $\text{C}_2\text{H}_3^+$  – were observed and six dissociation channels –  $c\text{-C}_2\text{H}_4\text{S}^+ \rightarrow \text{CH}_3\text{CS}^+ + \text{H}$ ,  $\text{HCS}^+ + \text{CH}_3$ ,  $\text{H}_2\text{S}^+ + \text{C}_2\text{H}_2$ ,  $\text{C}_2\text{H}_3^+ + \text{HS}$ ,  $\text{CH}_2\text{CS}^+ + \text{H}_2$  and  $\text{CHCSH}^+ + \text{H}_2$  – were established.

As the dissociation channel  $c\text{-C}_2\text{H}_4\text{S}^+ \rightarrow \text{CH}_3\text{CS}^+ + \text{H}$  of least energy likely involves structural alternation during dissociation, we expected substantial kinetic energies released on the dissociation if reverse activation barriers exist. Our PIMS results also show that a previous proposition of formation of an angular structure of  $\text{HCS}^+$  needs to be revisited. Accordingly, the combination of TPEPICO experiments on measurements of kinetic energies releases with the aid of G3 calculations should help us understand the detailed dissociation mechanisms.

Figures 1(a)-(e) show the coincidence TOF spectra of  $c\text{-C}_2\text{H}_4\text{S}$  excited at 9.06, 10.83, 10.88, 10.98 and 11.04 eV; solid lines indicate TOF peaks fitted to Gaussian shapes. The TOF peak of  $c\text{-C}_2\text{H}_4\text{S}^+$  fitted to a Gaussian profile has a full width at half maximum (fwhm) 26 ns; accordingly the transverse temperature of the molecular beam is calculated to be 10 K. This result indicates a small transverse velocity of the skimmed molecular beam along the detection axis and negligible  $c\text{-C}_2\text{H}_4\text{S}^+$  signals resulting from thermal (298 K) background that would broaden a TOF peak.

In Figs. 1(b)-(e), a well-resolved and symmetrically broadened TOF peak of fragment ion  $\text{C}_2\text{H}_3\text{S}^+$  is also observed; the broadened TOF peak indicates release of kinetic energy upon dissociation and was fitted well to a Gaussian shape. Among the stable  $\text{C}_2\text{H}_3\text{S}^+$  isomers, predicted G3 dissociation energies for  $c\text{-C}_2\text{H}_4\text{S} \rightarrow \text{CH}_3\text{CS}^+ + \text{H}$ ,  $\text{CH}_2\text{CSH}^+ + \text{H}$ ,  $c\text{-C}_2\text{H}_3\text{S}^+ +$

$\text{H}$  are 10.51, 11.61 and 11.74 eV, respectively. Formation of  $\text{CH}_2\text{CSH}^+ + \text{H}$  and  $c\text{-C}_2\text{H}_3\text{S}^+ + \text{H}$  is thus excluded as their predicted dissociation energies 11.61 and 11.74 eV are much greater than the experimental AE value  $10.71 \pm 0.01$  eV determined in the PIMS experiments.  $\text{CH}_3\text{CS}^+$  is the most likely structure on energetic grounds despite a small difference 0.2 eV between the predicted and experimental values.

Figures 2(a)-(e) shows the coincidence TOF spectra of  $c\text{-C}_2\text{H}_4\text{S}$  excited at 11.13, 11.31, 11.50, 11.71 and 11.81 eV. As the photon energy increases, a broadened TOF peak of fragment ion  $\text{HCS}^+$  is observed in addition to those of  $c\text{-C}_2\text{H}_4\text{S}^+$  and  $\text{C}_2\text{H}_3\text{S}^+$ ; the broadening also reflects release of kinetic energy upon dissociation and was fitted well to a Gaussian shape.

For a distribution of this type, the average release of kinetic energy is related to the fwhm of the TOF peak and calculated from that fwhm according to the Maxwellian equation. Calculated average releases of kinetic energy for channels  $\text{HCS}^+ + \text{CH}_3$  and  $\text{CH}_3\text{CS}^+ + \text{H}$  are depicted as circles in Figs. 3(a)-(b), respectively. Quasi-equilibrium theory (QET) calculations were also performed according to an equation formulated by Klots and plotted in the figures for a comparison. For channel  $\text{HCS}^+ + \text{CH}_3$ , our linearly extrapolated threshold at  $10.99 \pm 0.04$  eV agrees satisfactorily with a predicted G3 dissociation energy 11.05 eV for formation of linear  $\text{HCS}^+$  and  $\text{CH}_3$ . And also the QET results fit well the experimental data near the dissociation threshold although significant differences are observed at greater photon energies. These results imply that the energy for isomerization of  $c\text{-C}_2\text{H}_4\text{S}^+$  into the dissociation precursor lies below or near the dissociation threshold because formation of  $\text{HCS}^+$  and  $\text{CH}_3$  likely involves H migration before dissociation occurs.

For channel  $\text{CH}_3\text{CS}^+ + \text{H}$ , as seen in Fig 3(b), the measured releases of kinetic energy are substantial, but the results of QET calculations lie far below experimental values. A non-statistical kinetic energy distribution indicates that dissociation occurs through a dissociative excited state or involves substantial exit barriers. The presence of substantial exit barriers is likely due to H migration and structural

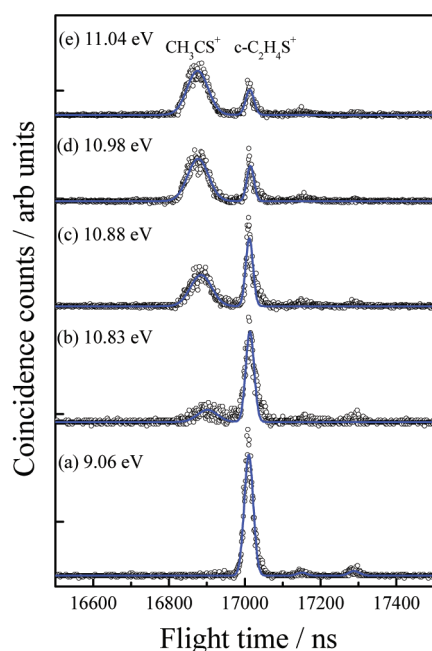


**Fig. 1:** Coincidence TOF spectra of  $c\text{-C}_2\text{H}_4\text{S}$  excited at photon energies (a) 9.06, (b) 10.83, (c) 10.88, (d) 10.98, and (e) 11.04 eV.

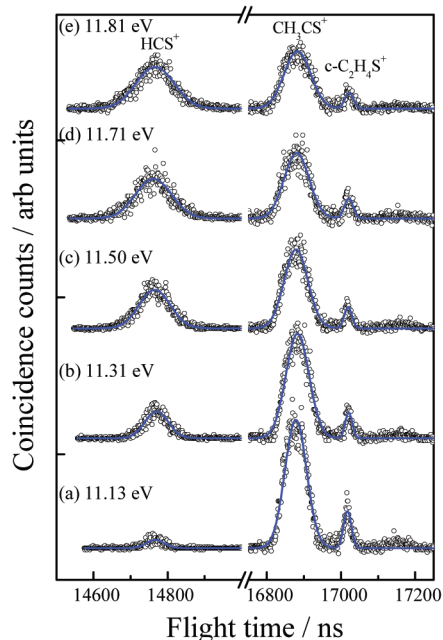


**Fig. 2:** Coincidence TOF spectra of  $c\text{-C}_2\text{H}_4\text{S}^+$  excited at photon energies (a) 11.13, (b) 11.31, (c) 11.50, (d) 11.71, and (e) 11.81 eV.

alternations during dissociation. In contrast, the existence of a dissociative excited state is excluded because there is no electronic state but a Franck-Condon gap in a region  $\sim 10.0 - 10.7$  eV according to photoelectron spectrum. Moreover, an impulsive model is generally applied to the dissociation that proceeds rapidly from a repulsive dissociative potential energy surface, but our calculations based on an impulsive model do not fit well the experimental data.

To further elucidate the detailed dissociation mechanisms, we explored the dissociation mecha-

nisms for channels  $\text{HCS}^+ + \text{CH}_3$  and  $\text{CH}_3\text{CS}^+ + \text{H}$  with the G3 method. Figure 4 shows the predicted relative energies of a feasible dissociation mechanism. For channel  $\text{CH}_3\text{CS}^+ + \text{H}$ ,  $c\text{-C}_2\text{H}_4\text{S}^+$  undergoes H migrations, ring opening and C–S bond breaking via transition states – TS1, TS2, and TS3 – to form  $\text{CH}_3\text{CSH}^+$  (LM3). In further formation of the most stable isomer  $\text{CH}_3\text{CHS}^+$  (1),  $\text{CH}_3\text{CSH}^+$  (LM3) subsequently proceeds H migration from the SH group to the central C atom via TS4. As dissociation of  $\text{CH}_3\text{CHS}^+$  (1) to form  $\text{CH}_3\text{CS}^+ + \text{H}$  involves only direct cleavage of the C–H bond, one would expect to find a completely statistical distribution of energy, which is not observed in our experiments. In contrast, if dissociation of  $\text{CH}_3\text{CSH}^+$  (LM3) via TS4 to form  $\text{CH}_3\text{CS}^+ + \text{H}$  takes place, substantial kinetic energies are expected to be released during dissociation, compatible with experimental observations. In addition, the predicted barrier of TS4 at 1.74 eV agrees with a difference 1.66 eV between the experimental AE 10.71 eV and IE 9.05 eV determined in previous PIMS studies. We sought to break the C–S bond directly to form a ring-opened structure  $\text{CH}_2\text{CH}_2\text{S}^+$ , but located no transition state for this process. Despite of a smaller barrier 1.87 eV predicted for isomerization of  $c\text{-C}_2\text{H}_4\text{S}^+$  into  $\text{CH}_2\text{SCH}_2^+$ , this dissociation mechanism is unexpected because of the weakness of the C–S bond relative to the C–C bond.

For channel  $\text{HCS}^+ + \text{CH}_3$ , the dissociation of  $\text{CH}_3\text{CHS}^+$  (1) to form  $\text{HCS}^+ + \text{CH}_3$  proceeds through direct cleavage of the C–C bond without an exit barrier and would result in a statistical energy distribution in the dissociation. Also, a predicted G3 barrier 1.94 eV for isomerization of  $c\text{-C}_2\text{H}_4\text{S}^+$  to  $\text{CH}_3\text{CHS}^+$  (1) is nearly the same as a predicted dissociation energy 1.99 eV. These results agree satisfactorily with our experimental observations.

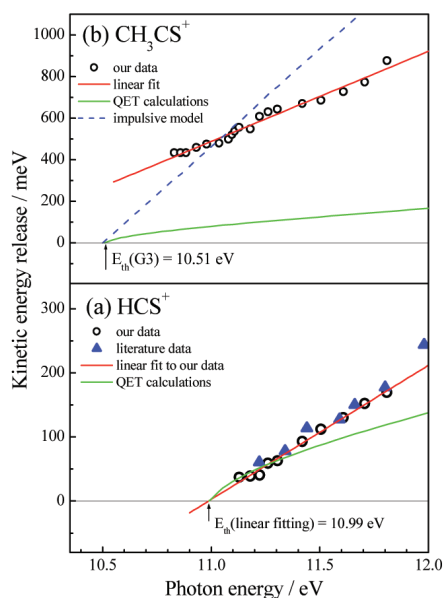
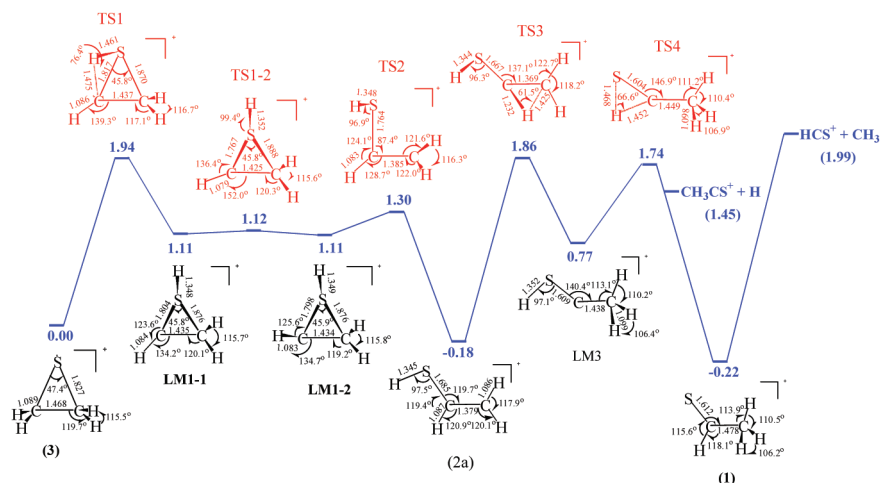


**Fig. 3:** Average kinetic energy released into dissociation channels  $c\text{-C}_2\text{H}_4\text{S}^+ \rightarrow$  (a)  $\text{HCS}^+ + \text{CH}_3$  and (b)  $\text{CH}_3\text{CS}^+ + \text{H}$  with excitation at photon energies in a region 10.6–11.8 eV. Data, a line fitted to data, QET calculations, and a calculation according to an impulsive model are marked as circles, solid line, dashed line and dotted line, respectively; literature data in Fig. 3(a) are marked as solid triangles for comparison.

**Fig. 4:** Theoretical predictions of relative energies in eV for isomerization of  $c\text{-C}_2\text{H}_4\text{S}^+$  into  $\text{CH}_3\text{CHS}^+$  before dissociation into channels  $\text{CH}_3\text{CS}^+ + \text{H}$  and  $\text{HCS}^+ + \text{CH}_3$ ; bond lengths in Å and interbond angles in degrees are indicated for molecular structures optimized at the MP2(full)/6-31G(d) level.



In conclusion, we reported the dissociation mechanisms of  $c\text{-C}_2\text{H}_4\text{S}^+$  to form  $\text{CH}_3\text{CS}^+ + \text{H}$  and  $\text{HCS}^+ + \text{CH}_3$  based on the results of TPEPICO experiments and G3 calculations. A predicted energy profile for isomerization of  $c\text{-C}_2\text{H}_4\text{S}^+$  into the dissociation precursors  $\text{CH}_3\text{CSH}^+$  and  $\text{CH}_3\text{CHS}^+$  supports the experimental results. The author thanks the National Science Council of Taiwan for financial support of this research.

### Experimental Station

Molecular beam/threshold photoelectron-photoion coincidence end station

### Publications

- Y.-S. Fang, I-Feng Lin, Y.-C. Lee, and S.-Y. Chiang, *J. Chem. Phys.* **123**, 054312 (2005).
- S.-Y. Chiang and Y.-S. Fang, *J. Electron Spectrosc. Relat. Phenom.* **144-147**, 223 (2005).

### Contact E-mail

[schiang@nsrrc.org.tw](mailto:schiang@nsrrc.org.tw)